

## RESEARCH AND EDUCATION

# Finite element modeling of an intact and cracked mandibular second molar under quantitative percussion diagnostics loading

Jie Shen, PhD,<sup>a</sup> Nasrin Taheri-Nassaj, PhD,<sup>b</sup> Cherilyn G. Sheets, DDS,<sup>c</sup> and James C. Earthman, PhD<sup>d</sup>

Percussion has been used qualitatively in medical and dental practice for over 200 years.<sup>1,2</sup> Percussion diagnostics has become a standard approach in physical examination in medicine. In dentistry, the dental mirror handle has been used as a dental percussion tool for qualitatively determining the stability of a tooth or implant. A quantitative percussion device (Perimeter; Perimetrics Inc) that demonstrated the ability to characterize the presence of cracks and defects as well as the mechanical integrity of underlying bone was introduced in 2002 (Fig. 1).<sup>3-9</sup> The hand-held probe is used to lightly tap the patient's tooth or dental implant. The probe contains a force sensor in a stainless-steel rod that accelerates to a predetermined velocity just before it taps the specimen and records the resultant force as a function of time. Further details on the operation of this system have been reported.<sup>3,4</sup>

### ABSTRACT

**Statement of problem.** Quantitative percussion diagnostics (QPD) has been devised to nondestructively evaluate the mechanical integrity of human teeth and implants, the mechanical integrity of the underlying bone, and the presence of cracks, but the mechanism is not clearly understood.

**Purpose.** The purpose of this study is to better understand the dynamic behavior of a tooth under conditions consistent with QPD by focusing on physiologically accurate 3D finite element models of a human mandibular second molar with surrounding tissues.

**Material and methods.** Finite element analysis (FEA) was used to study the force response of dental structures measured by the sensor in a QPD handpiece. A defect-free (intact) and a cracked tooth model containing a vertical crack involving enamel, dentin, periodontal ligament, bone, and the QPD percussion rod were used for this purpose. Different crack gap spaces were studied for comparison. The FEA model was validated with clinical QPD data for a second mandibular molar containing a vertical crack that subsequently had to be extracted. The location and size of the vertical crack was determined once the tooth was extracted.

**Results.** The present FEA results exhibited features consistent with those of corresponding clinical data, thus verifying the model. An examination of the relative acceleration of the crack faces with respect to each other revealed that an oscillation between the crack surfaces results in secondary peaks in the QPD energy return response compared with that of an intact tooth.

**Conclusions.** The present FEA modeling can generate simulated QPD results that exhibit established distinguishing characteristics in clinical QPD data for intact and cracked second mandibular molars. The model results also give insight into how QPD detects the presence of cracks and show that the oscillation of crack surfaces can produce the multipeak QPD results for a cracked molar observed clinically. (J Prosthet Dent xxxx;xxx:xxx-xxx)

Cracks in teeth are often not resolvable visually or with a radiograph.<sup>10</sup> An advanced crack is occasionally detected during clinical evaluation with an explorer or identified by a change in color because of shadowing at the area of

Supported by Perimetrics, Inc. [Research Agreement No. 211102]; 3D tooth geometries provided by eHuman, Inc.

Drs James Earthman and Cherilyn Sheets are the inventors of quantitative percussion diagnostics. They founded Perimetrics, Inc. following some of their research efforts with this technology and currently maintain a minority stock ownership in the company. Numerous patents have been issued and are pending. During the time the present research study was performed, Jie Shen was a PhD candidate at University of California, Irvine. He is currently employed by Perimetrics, Inc., a sponsor of the present research through a research agreement with the University of California, Irvine.

<sup>a</sup>PhD Candidate, Department of Materials Science and Engineering, University of California, Irvine, Irvine, Calif.

<sup>b</sup>Postdoctoral Researcher, Department of Materials Science and Engineering, University of California, Irvine, Irvine, Calif.

<sup>c</sup>Co-Executive Director, Research and Teaching Divisions, Newport Coast Oral Facial Institute, Newport Beach, Calif.

<sup>d</sup>Professor, Department of Materials Science and Engineering, Department of Biomedical Engineering, University of California, Irvine, Irvine, Calif.

## Clinical Implications

The FEA simulation of an anatomically accurate 3D tooth model under percussion loading exhibited results with the same distinguishing characteristics as those observed in clinical data for an intact and cracked molar. It also showed that QPD can detect a vertical crack in a human molar because of oscillating crack surfaces.

fracture. Other nondestructive crack detection techniques include transillumination, magnification, dye penetrants, radiographs, occluding tests, and ultrasonography.<sup>5,6</sup> However, none of these methods have proven capable of reliably detecting cracks in teeth. For example, transillumination was only able to detect 42% of the cracks discovered under the microscope during destructive tooth disassembly.<sup>6</sup> By contrast, quantitative percussion diagnostics (QPD) was able to identify cracks and fractures in natural teeth as confirmed by a destructive exploratory tooth disassembly process performed under an optical microscope (98% agreement).<sup>5-9</sup> Crack detection by QPD was based on the observation that a single peak in mechanical energy returned to the percussion rod is produced as a function of time for an intact tooth, while for a cracked tooth this response can consist of multiple peaks. A normal fit error (NFE) parameter has been used to characterize this deviation in response shape from a single peak.<sup>6-9</sup>

Biomedical researchers often use finite element analysis (FEA) because it can substantially reduce research costs and lead time compared with only performing experiments or clinical trials. Working toward an accurate simulation of experimental results can also lead to an improved understanding of the physical mechanisms responsible for observed behavior. For example, results from finite element analysis models of



**Figure 1.** Quantitative percussion diagnostics research instrumentation manufactured by Perimetrics, Inc.

intact (defect-free) teeth under percussion conditions provided insight into the properties and mechanical function of the periodontal ligament.<sup>11</sup> For validation, these simulations were compared with in vivo clinical QPD data for an intact molar.<sup>11</sup> In the present work, FEA was applied to both an intact and a cracked human mandibular second molar tooth under percussion loading to better understand why QPD results change so dramatically when a crack is present in a tooth.<sup>5-9</sup> The rationale for this investigation was that a finite element model and its results can be investigated in much more detail than is possible for a cracked tooth and QPD results in vivo. As such, a finite element model may provide additional insight as to the mechanics of a cracked tooth under percussion conditions. The research hypothesis was that percussion energy return response characteristics for a cracked molar observed in vivo using QPD can be predicted by a finite element model implemented with published material properties.

## MATERIAL AND METHODS

The present finite element models represented the structure of a single tooth complex and a QPD percussion rod.<sup>11</sup> Specifically, a tooth model of a human mandibular second molar was created (SOLIDWORKS; Dassault Systèmes SolidWorks Corp) using a tooth geometry data courtesy of eHuman, Inc. Mandibular second molars have 2 roots: a long mesial root and a slightly shorter distal root and are the longest roots relative to crown length of any human teeth.<sup>12</sup> The present models include enamel, dentin, an empty pulp chamber, the periodontal ligament (PDL), and surrounding bone as shown in [Figure 2](#). The PDL strongly binds the tooth root to the supporting bone, limits occlusal loads, and distributes the resulting stress over the hard tissues.<sup>11</sup> Bone has 2 distinct forms: cortical bone, and trabecular bone. However, this model only contains cortical bone, since previous studies have shown that the bone adjacent to teeth is typically cortical bone.<sup>4</sup> Commercially available codes (Marc and Mentat; MSC Software) were used for finite element analysis. The finite element tooth model was prepared in MSC Mentat as the pre- and postprocessor. MSC Marc, a nonlinear FEA solver was used because of its ability to model nonlinear material behaviors and transient environmental conditions, allowing for an accurate simulation under dynamic loading.

Tooth components have typically been modeled as linear elastic and isotropic materials.<sup>10</sup> The present study also considered the tooth, periodontal ligament, and neighboring bone as isotropic linear elastic materials. However, viscoelastic behavior was also simulated in the models based on Raleigh damping to properly incorporate the function of the PDL, dentin, and bone under percussion loading conditions. A detailed description of how Raleigh

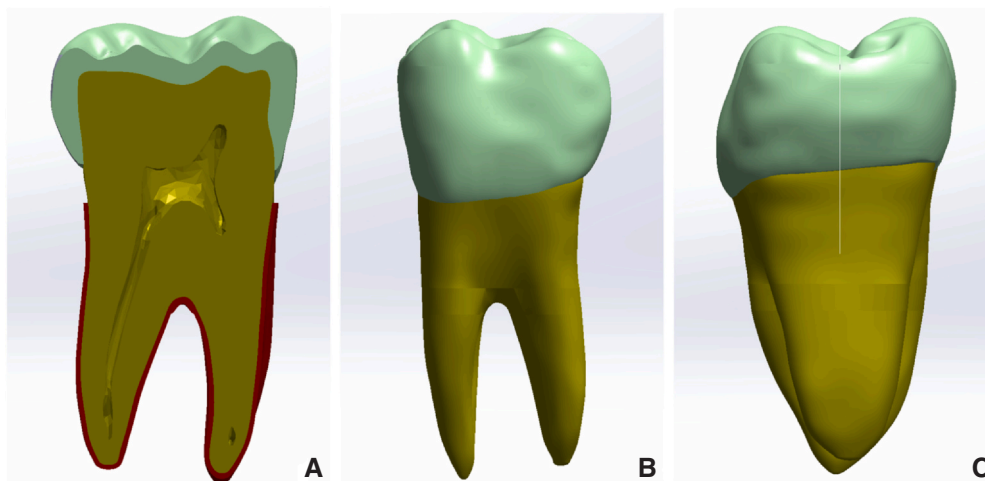


**Figure 2.** Different views of tooth geometry: A, Cross-section of intact tooth embedded in periodontal ligament. B, Buccal view of intact tooth. C, Buccal-lingual view of distal of same tooth containing 10-mm-long vertical crack.

**Table 1.** Properties of dental tissues<sup>11,13–16</sup>

Material	Young Modulus (MPa)	Poisson Ratio	Density (kg/m <sup>3</sup> )	Mass Matrix Multiplier	Stiffness Matrix Multiplier
Enamel	84 100; 50 000*	0.33	2970	0	0
Dentin	14 700	0.31	2410	0.0907	3×10 <sup>-5</sup>
Crack Tip Damage Zone (Dentin)	1470	0.31	2410	0.0907	3×10 <sup>-5</sup>
PDL	0.1; 0.03 <sup>a</sup>	0.45	1200	1814	0.6
Bone	14 700	0.3	1300	0.0907	3×10 <sup>-5</sup>

PDL, periodontal ligament.

\* Estimated value corresponding to bonded occlusal onlay shown in Figure 5.

<sup>a</sup> Estimated value for widened PDL shown in Figure 5.

damping was implemented in the present models has been described elsewhere.<sup>11</sup> The properties of dental system components including the elastic Young modulus, Poisson ratio, and mass density used in the present work are summarized in Table 1.<sup>11,13–16</sup> A damage zone was also incorporated into the FEA models containing a vertical crack. This damage zone was located at the vertical crack tip and had a Young modulus 10% of that for healthy dentin. The enamel component did not include a damage zone because of its suprabony location.

The operation of quantitative percussion testing was simulated using a 3-dimensional model of the tooth, periodontal ligament, surrounding bone, and percussion rod over a 0.4-ms period with 0.004-ms time increments. The stainless-steel percussion rod in the device handpiece had a Young modulus of 207 GPa and an initial velocity of approximately 60 mm/second. The resulting percussion force was predicted in the model at the piezoelectric sensor in the percussion rod to simulate the sensor's measurement.<sup>11</sup> The 3D model was anatomically accurate for a typical intact and vertical crack human mandibular second molar. The model had a total of over 1 million elements and is shown in Figure 3. Second order 0.1-mm isoperimetric 3-dimensional 10-node tetrahedron elements were used in the 0.2-mm-

thick PDL so that it contained at least 2 layers of elements.<sup>10</sup> Eight-node, isoperimetric, arbitrary hexahedral elements were used for the percussion probe, and linear isoperimetric 3-dimensional tetrahedron elements were used for the rest of the model. Boundary conditions were defined on the outer surfaces of the bone and percussion rod to prevent free body motion that would impact the data.

One of the most important applications of QPD is in the detection of cracks in teeth.<sup>5–9</sup> To understand better the mechanism of how QPD detects cracks, an *in vivo* mandibular second molar tooth was simulated with a crack extending from the occlusal surface vertically into the dentin. The vertical crack was 10 mm long, as illustrated in Figure 2, with a gap space between the crack surfaces of 20 μm. This gap space was within the range of those reported for microscopic examinations of cracks in extracted teeth. The length of this crack was modeled after a patient's cracked second mandibular molar that had been extracted immediately after being tested with QPD. A postextraction photograph of this tooth is shown in Figure 4 along with a corresponding x-ray image prior to extraction in Figure 5. For further verification of the present models, FEA simulations were compared with pre-extraction *in vivo* QPD clinical data

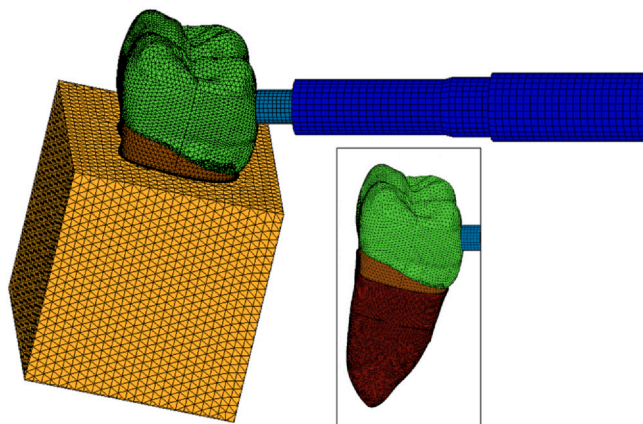


**Figure 3.** Complete finite element model used in present study in MSC Marc and Mentat software environments. Inset: Same view with bone removed.



**Figure 4.** Photograph of 10-mm-long vertical crack in extracted second mandibular molar. Dye penetrant can be seen in most of gap space of crack.

for the same cracked second mandibular molar. The FEA results for the cracked molar were then compared with those for an identical tooth model except that it was intact (crack-free).

QPD measures the resultant force returned by the tooth through a sensor in the tip of the percussion rod during the tapping process.<sup>3,4</sup> For these FEA models, plots of numerically determined resultant force produced at the sensor position in the rod tip and recorded as a function of time are used for the mathematical simulation of the percussion response of an intact and vertical cracked mandibular second molar. Force versus time plots obtained using QPD were compared with the FEA simulations to gain insight as to how QPD can sensitively detect the presence of cracks in teeth. To perform contact analysis in the present models, each part of the dental structure (enamel, dentin, PDL, and bone) was defined, and the percussion rod and the percussion rod tip were defined as deformable contact



**Figure 5.** Radiograph of second mandibular molar with 10-mm-long vertical crack shown in Figure 4. Occlusal onlay visible and bone defect shown on distal side, suggesting damaged PDL.

bodies. This structural specification made it possible to place contact surfaces at the location of the sensor in the rod tip and at the crack faces in the cracked molar model. The plot of contact area between 2 crack surfaces was obtained by performing a contact analysis. By tracking the contact area, it was possible to observe where crack closure had occurred. MSC MARC also allowed the selection of the contact area between 2 bodies as a post file value.

The results of the present FEA model were compared with the *in vivo* clinical QPD data for the molar containing a vertical crack with the same length, orientation, and location in the tooth. However, this clinical cracked tooth had previously received endodontic treatment, a porcelain onlay restoration, and a radiographic bone lesion with apparent damage to the PDL. Accordingly, the PDL Young modulus in the present FEA model was reduced to simulate the damaged PDL as noted in Table 1. In addition, the feldspathic porcelain onlay covering the occlusal surface was simulated by reducing the elastic modulus. The Young modulus range for feldspathic porcelain is reported to be 60 to 70 GPa.<sup>17</sup> The Young modulus of the adhesive bond between the restoration and tooth is much lower at about 2 GPa.<sup>18</sup> However, the bond's contribution to the effective modulus of the onlay should be substantially less than that for the porcelain Young modulus because of the relatively low volume fraction of adhesive in the tooth. Therefore, a lower Young modulus value of 50 GPa was used to simulate the presence of an onlay, as noted in Table 1. While it was not feasible to accurately measure these moduli for the extracted tooth, the goal of the present work was to determine whether the reduced moduli yielded simulated QPD results closer to the clinical QPD results obtained before extraction. It was also important to determine how much these changes in moduli altered the simulated value of NFE, which is



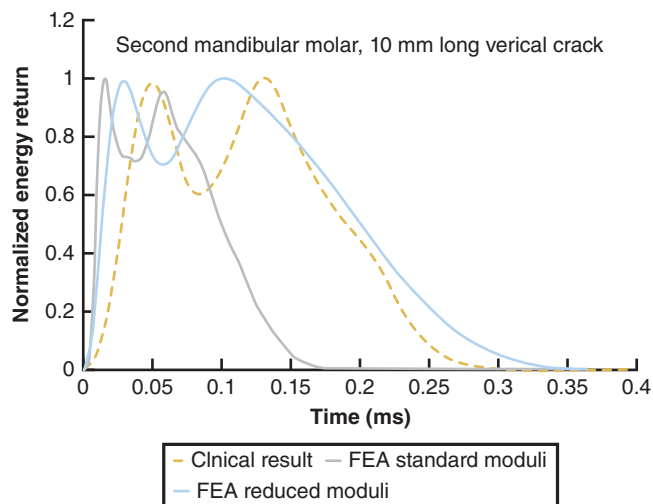


**Figure 6.** Comparison of clinical and FEA results on plot of normalized energy return versus time for tooth shown in Figure 4 prior to extraction. FEA results for both reported and reduced moduli for enamel and periodontal ligament shown. FEA, finite element analysis.

determined from the normalized energy return (NER) as a function of time for a tooth. The value of NER is related to percussion force according to

$$\text{NER} = \frac{F(t)^2}{F_{\max}^2},$$

where  $F(t)$  is the percussion force as a function of time and  $F_{\max}$  is the maximum force measured by the sensor in the handpiece rod during an entire percussion. The time dependence of the NER for a defect-free calibration sample can be approximated from

$$\text{NER} = \beta \exp[-(t - \phi)^2 / \psi],$$

where  $t$  is time, and  $\beta$ ,  $\phi$ , and  $\psi$  are constants that are determined by the best fit to the NER-time data. A

nonlinear regression fit of this equation to NER-time data was performed using the Levenberg-Marquardt algorithm.<sup>19</sup> The resulting mean residue, the weighted mean error of the fitted model to the entire data set, was calculated to obtain a normalized fit error (NFE).

## RESULTS

Figure 6 illustrates a comparison of normalized energy return as a function of time for the present FEA model and that for the pre-extraction clinical tooth shown in Figure 4. FEA results for both reported values of the tissue moduli and reduced moduli for the enamel and PDL are shown in this figure. A better match to the clinical data was achieved with a reduced Young modulus in the enamel portion of the tooth of 50 GPa and a reduced PDL Young modulus of 0.03 MPa. The match is reasonable given that the value of NFE for the clinical results is 0.054 and the NFE value for the FEA simulations is 0.058. These lower moduli are within reasonable ranges when the moduli of the restorative materials and the widened PDL shown in Figure 5 are considered.<sup>20</sup>

Figure 7 presents a plot of normalized energy return (NER) and percussion force as a function of time predicted by an FEA model corresponding to the force measured by the sensor in the percussion rod for an intact second mandibular molar (blue curve), that tooth containing a 10-mm-long vertical crack (green curve). The response for the molar containing a vertical crack contains multiple peaks as opposed to the predominantly single peak exhibited by the model for an intact (crack-free) mandibular second molar. This difference is consistent with clinical QPD responses obtained from intact and cracked teeth.<sup>3-9</sup>

The NFE value for the intact tooth model result in Figure 7 was 0.018, while a value of 0.058 was determined

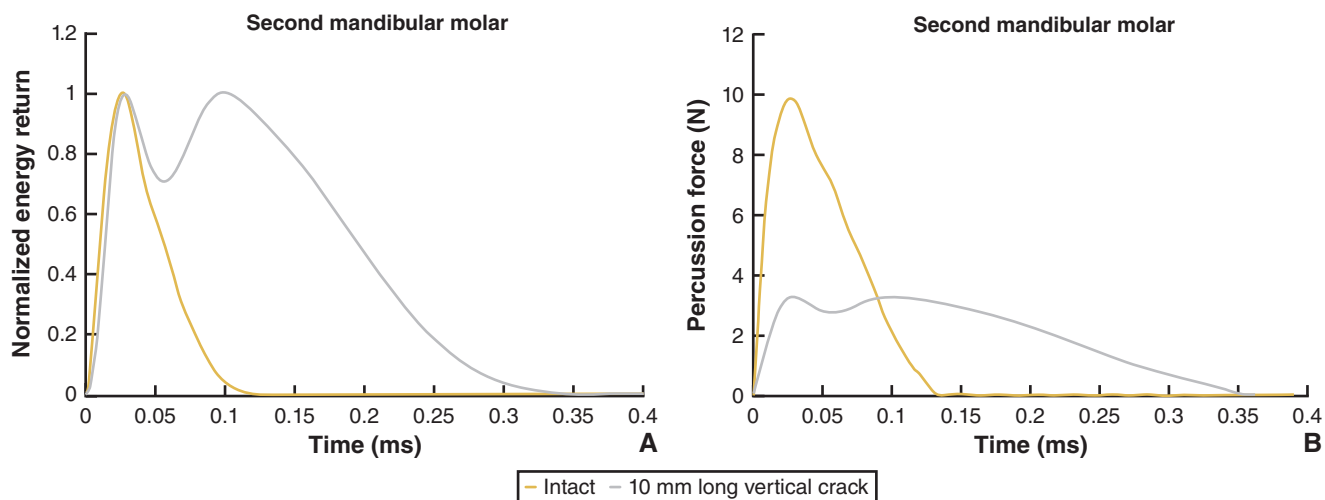


**Figure 7.** Predicted quantitative percussion diagnostics for intact mandibular second molar and same tooth containing 10-mm-long vertical crack with 10- $\mu\text{m}$  and 20- $\mu\text{m}$  gap spaces. A, Plotted as normalized energy return. B, Plotted as percussion force versus time.

for the cracked tooth model. Previous clinical studies reported that an NFE value of about 0.020 corresponds to the cross-over point from unlikely crack presence to the presence of a crack being probable (50% probability a crack is present).<sup>5,6</sup> For further comparison, NFE values were determined for the results of FEA models run with the normal Young modulus values listed in Table 1. For these models, the effects of the presence of an onlay and widened PDL in the clinical tooth were not considered. The resulting NFE value for the intact tooth was 0.005, and the value for the cracked molar was 0.034. Thus, omitting the effect of an onlay and widened PDL with lower modulus did not change the NFE based indication of a probable crack in the tooth for the cracked tooth FEA models.

Relative acceleration between the crack surfaces (black curve) was plotted as a function of time in Figure 8 and to the predicted measured percussion force versus time (green curve) for a 10-mm-long vertical crack in a mandibular second molar. The relative acceleration indicates how the crack surfaces are moving with respect to each other. The relative acceleration was determined by subtracting the acceleration of the lingual crack surface from the acceleration of the buccal crack surface. Since crack closure did not occur in the present models, contact between the crack surfaces did not cause or affect this acceleration. As indicated by the black arrows, there was a one-to-one correlation between peaks in the relative acceleration of the crack faces and peaks in the force response at the sensor region of the percussion rod. The small offset in these arrows corresponded to approximately 0.013 ms, suggesting that it takes a force wave this amount of time to propagate at the speed of sound from the crack tip region to the PDL and through the tooth to the sensor in the percussion rod. The correlation between the relative acceleration of the crack faces and measured force peaks indicates that a relatively high-frequency oscillation between the crack faces results in the

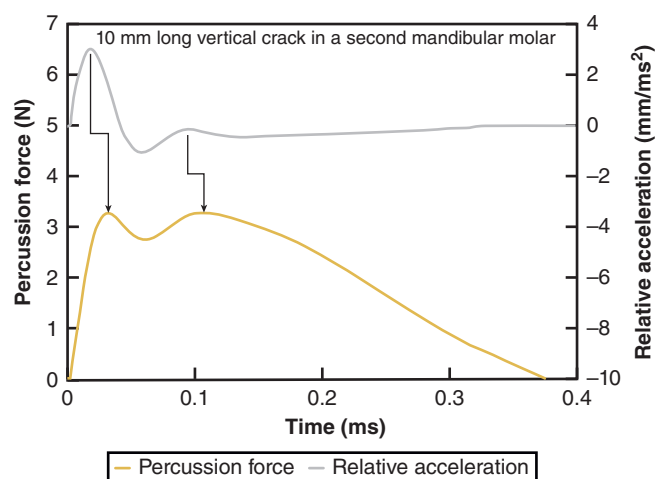


**Figure 8.** Force and relative acceleration versus time for 10-mm vertical crack with 20- $\mu$ m crack opening.

multiple peaks registered in the force data from the sensor in the percussion rod. In the absence of a crack, these peaks in the force response were not predicted by FEA as shown in Figure 5. This correlation between relative acceleration and measured force is to be expected considering that force is equal to the product of mass times acceleration. An estimate of the mass of the tooth on either side of the oscillating crack multiplied by the predicting acceleration yields values of force in the range of those predicted at the rod sensor.

## DISCUSSION

The present results did not support rejecting the research hypothesis that percussion energy return response characteristics for a cracked molar observed in vivo using QPD can be predicted by a finite element model implemented with published material properties. The overall shape of the FEA model result was similar to that for a clinical result when reductions in modulus values were taken into account. Differences in the shape of these curves may be attributed to different factors. For example, the crack dimensions were approximated after the extraction, which could further damage the tooth, and discrepancies in crack length and crack opening size may also exist. In addition, even though the FEA model uses a typical geometry of a mandibular second molar, minor variations may have been present in tooth size and geometry with respect to the clinical tooth. Despite these uncertainties, the present models were still able to capture the overall variation in the response from that for an intact tooth and an NFE value similar to that measured clinically. This similarity in distinguishing characteristics suggested that the NFE ability to indicate the presence of a crack is not very sensitive to these factors. Thus, the present FEA models were sufficiently accurate for depicting the changes in the NER responses that occur when a crack develops in a molar.

## CONCLUSIONS

Based on the findings of this finite element study, the following conclusions were drawn:

1. The FEA model was able to predict distinguishing characteristics of a QPD response for a cracked molar when elastic and damping properties in the range of those reported in the scientific literature were used.
2. Those characteristics were multiple peaks resulting from the presence of a crack and NFE values in the ranges of those reported in earlier studies for intact and cracked teeth.
3. Comparison of the relative acceleration between crack faces with simulated sensor measurements indicated that the multiple peaks observed in the

clinical QPD data for a molar containing a crack are caused by an oscillation of the crack surfaces.

## REFERENCES

1. Bynum WF. *Science and the Practice of Medicine in the Nineteenth Century*. New York: Cambridge University Press; 1994.
2. Bennion E. *Antique Medical Instruments*. 1st ed... California: University of California Press; 1979.
3. Dinh A, Sheets CG, Earthman JC. Analysis of percussion response of dental implants in an in vitro study. *Mater Sci Eng C Mater Biol Appl*. 2013;33:2657–2663.
4. Sheets CG, Hui DD, Bajaj V, Earthman JC. Quantitative percussion diagnostics and bone density analysis of the implant-bone interface in a pre- and postmortem human subject. *Int J Oral Maxillofac Implants*. 2013;28:1581–1588.
5. Sheets CG, Stewart DL, Wu JC, Earthman JC. An in vitro comparison of quantitative percussion diagnostics with a standard technique for determining the presence of cracks in natural teeth. *J Prosthet Dent*. 2014;112:267–275.
6. Sheets CG, Wu JC, Rashad S, Phelan M, Earthman JC. In vivo study of the effectiveness of quantitative percussion diagnostics as an indicator of the level of the structural pathology of teeth. *J Prosthet Dent*. 2016;116:191–199.
7. Sheets CG, Wu JC, Earthman JC. In vivo study of quantitative percussion diagnostics as an indicator of the level of the structural pathology of teeth: Retrospective follow-up investigation of high risk sites that remained pathological following restorative treatment. *J Prosthet Dent*. 2018;119:928–934.
8. Sheets CG, Wu JC, Zhang L, Earthman JC. Ten-year retrospective study of the effectiveness of quantitative percussion diagnostics as an indicator of the level of structural pathology in teeth. *J Prosthet Dent*. 2020;123:693–700.
9. Sheets CG, Quan DA, Wu JC, Earthman JC. An evaluation of quantitative percussion diagnostics for determining the probability of a microgap defect in restored and unrestored teeth: A prospective clinical study. *J Prosthet Dent*. 2023;154:235–244.
10. Ferracane JL, Hilton TJ, Funkhouser E. National Dental Practice-Based Research Network Collaborative Group. Lessons learned from the cracked tooth registry: A 3-year clinical study in the nation's network. *J Am Dent Assoc*. 2023;154:235–244.
11. Mapar A, Taheri-Nassaj N, Shen J, Komari O, Sheets CG, Earthman JC. Finite element study of periodontal ligament properties for a maxillary central incisor and a mandibular second molar under percussion conditions. *J Med and Biol Eng*. 2022;42:681–691.
12. Scheid RC. *Woelfel's Dental Anatomy: Its Relevance to Dentistry*. 7th ed... Philadelphia: Lippincott Williams Wilkins; 2007:120–163.
13. O'Brien W. *Dental materials and their election*. 4th ed... Hanover: Quintessence Publishing Company; 2008:335.
14. Poppe M, Bourauel C, Jäger A. Determination of the elasticity parameters of the human periodontal ligament and the location of the center of resistance of single-rooted teeth. A study of autopsy specimens and their conversion into finite element models. *J Orofac Orthop*. 2002;63:358–370.
15. Fill TS, Carey JP, Toogood RW, Major PW. Experimentally determined mechanical properties of, and models for, the periodontal ligament: Critical review of current literature. *J Dent Biomech*. 2011;2011:312980.
16. Farah W, Craig RG, Meroueh KA. Finite element analysis of a mandibular model. *J Oral Rehab*. 1988;15:615–624.
17. Ruales-Carrera E, Dal Bó M, Fernandes das Neves W, Fredel MC, Maziero Volpato CA, Hotza D. Chemical tempering of feldspathic porcelain for dentistry applications: A review. *Open Ceramics*. 2022;9:100201.
18. Giannini M, Mettenburg D, Arrais CA, Rueggeberg FA. The effect of filler addition on biaxial flexure strength and modulus of commercial dentin bonding systems. *Quintessence Int*. 2011;42:e39–e43.
19. Nocedal J. *Wright, Numerical optimization*. 2nd ed... Springer Series in Operations Research; 2006.
20. Natali AN. *Dental biomechanics*. 1st ed... London: CRC Press; 2003.

### Corresponding author:

Dr Jie Shen  
Perimetrics, Inc.  
8441 154th Avenue NE  
Building H, Suite 210  
Redmond, WA 98052  
Email: shenj8@uci.edu

### Acknowledgments

The authors thank MSC Software, a division of Hexagon Inc., for licenses to use the Marc and Apex codes, as well as Doug Malcolm (MSC Software) and Dr David Dimas (UC Irvine) for their assistance with these codes. The authors also thank Drs Eric Herbranson, Bao Pham, and Kevin Montgomery for their assistance in obtaining 3D tooth geometries from eHuman.

### CRediT authorship contribution statement

**Jie Shen:** Writing- original draft, Conceptualization, Methodology, Formal analysis, Investigation, Visualization, Validation, Data curation, Writing – review and editing. **Nasrin Taheri-Nassaj:** Conceptualization, Methodology, Investigation, Writing – original draft, Visualization. **Cherilyn G. Sheets:** Supervision, Validation, Resources, Data Curation, Investigation, Writing – reviewing and editing. **James C. Earthman:** Supervision, Resources, Conceptualization, Funding acquisition, Writing – reviewing and editing, Project administration.

Copyright © 2024 by the Editorial Council of *The Journal of Prosthetic Dentistry*. All rights are reserved, including those for text and data mining, AI training, and similar technologies.

<https://doi.org/10.1016/j.prosdent.2024.09.003>